CrossMark

Near-infrared laser scanning confocal microscopy and its application in bioimaging

Chaowei Sun[1] · Yalun Wang[1] · Hequn Zhang[1] · Jun Qian[1]

Abstract Near-infrared (NIR) fluorescence imaging is an important imaging technology in deep-tissue biomedical imaging and related researches, due to the low absorption and scattering of NIR excitation and/or emission in biological tissues. Laser scanning confocal microscopy (LSCM) plays a significant role in the family of fluorescence microscopy. Due to the introduction of pinhole, it can provide images with optical sectioning, high signal-to-noise ratio and better spatial resolution. In this study, in order to combine the advantages of these two techniques, we set up a fluorescence microscopic imaging system, which can be named as NIR-LSCM. The system was based on a commercially available confocal microscope, utilizing a NIR laser for excitation and a NIR sensitive detector for signal collection. In addition, NIR fluorescent nanoparticles (NPs) were prepared, and utilized for fluorescence imaging of the ear and brain of living mice based on the NIR-LSCM system. The structure of blood vessels at certain depth could be visualized clearly, because of the high-resolution and large-depth imaging capability of NIR-LSCM.

Keywords Near-infrared (NIR) · Laser scanning confocal microscopy (LSCM) · NIR nanoparticles (NPs) · In vivo · Bioimaging

1 Introduction

Fluorescence imaging in the optical tissue window of 700–900 nm (a commonly used NIR spectral region) can provide larger imaging depth and better signal-to-noise ratio compared to traditional fluorescence bioimaging in visible spectral region, due to lower light scattering and absorption (Welsher et al. 2011; Weissleder 2001; Tao et al. 2012; Luo et al. 2011; Kim et al. 2012). In addition, since autofluorescence from biological tissues in NIR

✉ Jun Qian
  qianjun@zju.edu.cn

[1] State Key Laboratory of Modern Optical Instrumentation, Centre for Optical and Electromagnetic Research, Zhejiang University, Hangzhou 310058, China

region is not so distinct, NIR fluorescence bioimaging can provide fine signal-to-background ratio (Weissleder 2001; Owens et al. 2015; Welsher et al. 2008). Furthermore, long-wavelength excitation light is usually adopted in NIR fluorescence bioimaging, which owns lower photon energy compared to the short-wavelength excitation light in visible fluorescence bioimaging, producing less damage towards bio-samples (Uh and Petoud 2010). However, NIR fluorescence imaging is usually performed on the wide-field mode where a camera lens is used to collect the images, and its spatial resolution is usually limited.

Laser scanning confocal microscopy (LSCM) is a typical modality in the family of microscopy. Thanks to the spatial filtering effect of a pinhole placed at the confocal plane of the lens, out-of-focus signal light can be eliminated, rendering LSCM with optical sectioning, high signal-to-noise ratio and better spatial resolution (Ntziachristos 2010; Hardham 2012). LSCM has been widely applied in biomedical researches (Yang et al. 2005; Webb 1996). However, since the excitation wavelength of LSCM usually locates in the visible spectral region, its penetration capability in thick biological samples is restricted due to light scattering and water absorption. Thus, LSCM is mainly adopted in cell imaging and thin tissue imaging. Recently, LSCM based on NIR reflecting has been utilized for clinical applications (e.g. human skin imaging, http://www.vivascope.de/en/products.html). In 2014, our group utilized LSCM for in vivo fluorescence imaging, with the assistance of NIR emitted polymer nanoparticles (NPs), and achieved three-dimensional (3D) reconstruction of the cerebral vasculatures of a mouse as deep as 500 μm (Chu et al. 2014). Nevertheless, the study still has some room for further improvement. The excitation light was from a red emitted laser ($\lambda = 635$ nm), which was near but not within the "optical tissue window" of 700–900 nm (Yodh and Chance 1995; Huang et al. 2006; Shi Kam et al. 2005; Welsher et al. 2009; Diev et al. 2012), and its attenuation in tissues was distinct. 635-nm excitation was also far from the absorption peak (831 nm) of the NIR NPs, and the fluorescence intensity of the NPs was actually not so strong. In addition, the fluorescence detector photomultiplier tube (PMT) was visible but not NIR sensitive and the detection efficiency could be optimized further.

In this study, to fully take advantages of the deep-tissue penetration capability of NIR fluorescence imaging and the optical sectioning of LSCM, we established a NIR-LSCM system. It was based on a commercially available confocal microscope, utilizing a NIR laser as the excitation ($\lambda_{ex} = 785$ nm) and a NIR sensitive PMT as the detector. Compared with traditional LSCM system, the new NIR-LSCM system has some advantages. The first is the improvement of imaging depth, because of the lower light scattering and absorption of NIR excitation and emission in tissues. The second is the improvement of signal-to-background ratio, due to the much lower autofluorescence from bio-tissues under NIR excitation. The third is the reduced photo-damage to bio-samples, as NIR excitation has lower single photon energy than visible and ultraviolet excitation. In our experiment, we chose ICG (Indocyanine green) as the NIR fluorescent dye, which has been approved by Food and Drug Administration (FDA) of USA for clinical use (Treger et al. 2014; Liu et al. 2017; Kim et al. 2015; Ryeom et al. 2004). ICG molecules were encapsulated with amphiphilic polymers to form NPs. The absorption and fluorescence peaks of ICG NPs both located in the "optical tissue window" of 700–900 nm. Under 785 nm excitation, they gave out bright NIR fluorescence, which was beneficial for deep-tissue bioimaging. The glass capillary filled with the aqueous dispersion of ICG NPs was observed with the NIR-LSCM system, and bright NIR fluorescence images were obtained, which verified their feasibility as fluorescent probes for NIR-LSCM. Subsequently, the NIR-LSCM system was utilized for in vivo bioimaging study. ICG NPs was intravenously injected into the

mice via tail vein, and 3D reconstructed images of ear blood vessels (depth = 200 μm) and cerebral blood vessels (depth = 500 μm) in living mice were achieved successfully. NPs assisted NIR-LSCM is very promising for deep-tissue and high-resolution in vivo bioimaging.

2 Experiments

2.1 NIR-LSCM system

The NIR-LSCM system was set up based on a commercial microscope (Olympus, FV 1000 + BX61). As showed in Fig. 1, the beam from a NIR semiconductor laser centered at 785 nm was introduced into the microscope by a light climbing system (consisted of two mirrors). After that, the light was reflected by dichroic mirror 1 (DM 1), dichroic mirror 2 (DM 2) and mirror 1 (M 1), and reached dichroic mirror 3 (DM 3, 800 nm long-pass). The 785-nm light beam was reflected by DM 3, and further reflected by the two mirrors in the galvanometer system, which was used to realize the scanning in X–Y axis. After passing through the scan lens and tube lens respectively, the beam was reflected by mirror 2 (M 2) and focused on the sample with a water-immersed objective (20X, NA = 1, work distance: 2 mm, Olympus). The power of the 785 nm light after objective was ∼ 6 mW. NIR fluorescence signals were collected by the same objective. They were then reflected by M 2, and passed through the tube lens, scan lens and galvanometer. The fluorescence within 800 nm was cut-off by DM 3, and the fluorescence beyond 800 nm could pass. The fluorescence signals reached the pinhole after reflected by mirror 3 (M 3) and mirror 4 (M
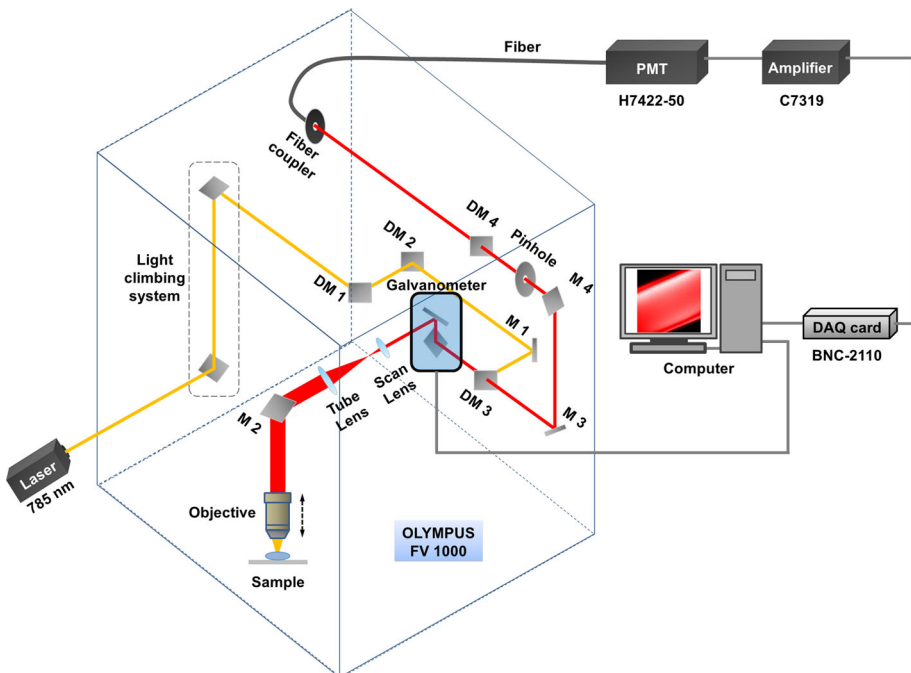
Fig. 1 Schematic illustration of the NIR-LSCM system. DM stands for dichroic mirror, M stands for mirror

4). After spatially filtered by the pinhole, the NIR signals were spectrally filtered by DM 4 (Semrock, an 800 nm long-pass dichroic mirror, LPD02-785RU) to get rid of the residual 785 nm excitation light. Finally, the NIR fluorescence signals were coupled into a fiber and collected by the PMT (Hamamatsu, H7422-50), which was sensitive to the weak light signal of 380–890 nm and had an optimal sensitivity around 800 nm. The electrical response from PMT was amplified by C7319 (Hamamatsu) and then collected by a data acquisition card (DAQ card, National Instrument, NBC-2110), which was connected to a computer. With the synchronization of galvanometer scanning and DAQ card recording (controlled by the same computer), a NIR fluorescence image could be obtained and displayed on the computer. Moreover, by micro-moving the objective to various z depths, fluorescence images at different depths could be obtained, and a three-dimensional imaging could be realized via software processing.
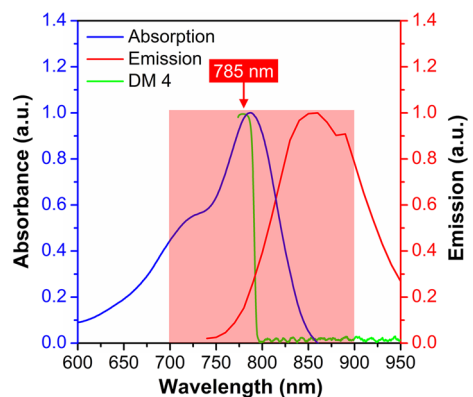
2.2 NIR fluorescent NPs

Amphiphilic polymer DSPE-mPEG$_{5000}$ was introduced to encapsulate ICG molecules, in order to obtain more stable and biocompatible NIR fluorescent NPs with longer blood circulation time. Typically, 500 μL of ICG in chloroform (500 μm) was mixed with 2 mL of DSPE-mPEG$_{5000}$ in chloroform (10 mg mL^{-1}). The mixture was sonicated and then dried in a rotary vacuum evaporator. Followed, 500 μL PBS (1X, pH = 7.4) was added into the lipidic film and the dispersion was sonicated to be homogeneous. In this way, ICG doped polymer NPs were obtained, which could be used for further experiments.

3 Results and discussion

3.1 Optical properties of ICG NPs

The absorption spectrum of ICG NPs in aqueous dispersion was measured with a spectrophotometer (Shimadzu, UV-2550), and the fluorescence spectrum of ICG NPs was measured with the Maestro in vivo optical imaging system (CRI, Inc. Woburn, MA), with the excitation wavelength of 704 nm. As shown in Fig. 2, ICG NPs had distinct absorption in the range of 700–800 nm (in blue), which located in the "optical tissue window" of 700–900 nm. As a result, the laser with its wavelength at 785 nm can effectively excite the


Fig. 2 Normalized absorption spectrum (blue) and normalized fluorescence spectrum (red) of ICG NPs in aqueous dispersion. The green line indicates the absorption spectrum of 800 nm long-pass dichroic mirror (DM 4). The pink region indicates the "optical tissue window" of 700–900 nm. Excitation wavelength (785 nm) and most fluorescence signals locate in the window. (Color figure online)

NIR fluorescence of ICG NPs. In addition, ICG NPs had NIR emission in the range of 800–900 nm (in red), which also located in the "optical tissue window" of 700–900 nm and could be detected by H7422-50 PMT effectively. Thus, during the NIR-LSCM imaging, DM 3 (800 nm long-pass) was used to separate NIR signals from the 785 nm-excitation and DM 4 (800 nm long-pass, in green) was able to filter away the residual 785 nm-excitation light effectively.

3.2 NIR-LSCM imaging of a glass capillary filled with ICG NPs

Prior to in vivo bioimaging study, we employed the NIR-LSCM system for the imaging of ICG NPs in a glass capillary. The scanning speed was 10 μs pixel^{-1} (512 × 512 pixels per frame). Figure 3 shows the NIR microscopic images of ICG NPs (in aqueous dispersion, the concentration of net ICG was 500 μm) at different vertical layers of the glass capillary. Based on these images, a 3D reconstruction was built (Fig. 3l). The NIR signals from the ICG NPs were strong, endowing the images with high contrast. In addition, thanks to the confocal design in our NIR-LSCM system, the obtained images showed high resolution. The experimental results preliminarily verified the feasibility of ICG NPs in the subsequent in vivo imaging applications.
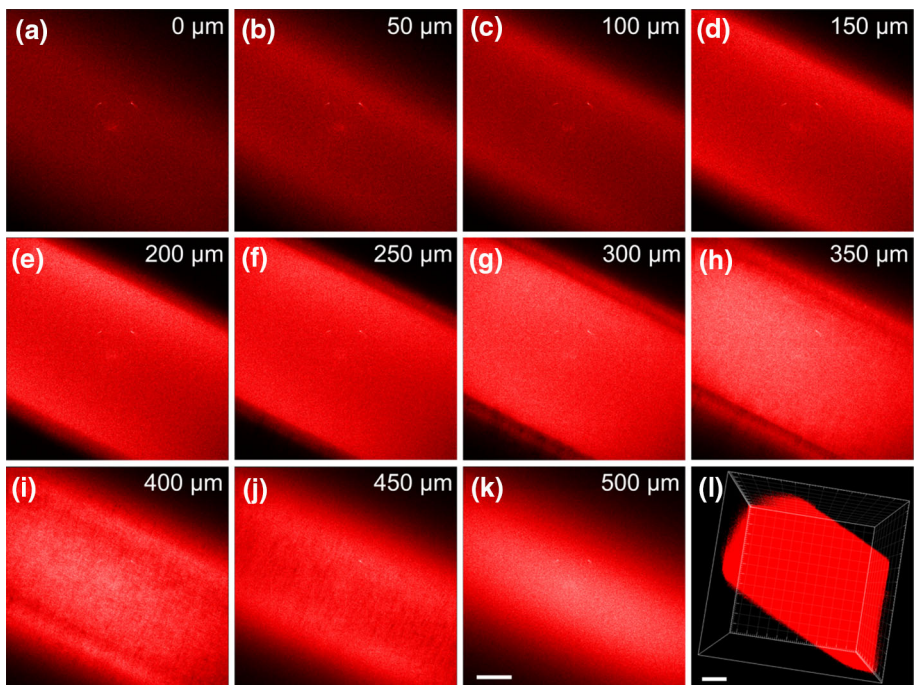

Fig. 3 NIR-LSCM images of a glass capillary filled with aqueous dispersion of ICG NPs (500 μm) at various depths **a–k** 0–500 μm. **l** A 3D reconstructed image shows the distribution of ICG NPs in the glass capillary. Scale bar: 100 μm

## 3.3 NIR-LSCM imaging of the ear blood vessels in a living mouse

The NIR-LSCM system was then utilized for in vivo bioimaging. 8-week-aged female ICR mice anesthetized with pentobarbital were injected with PBS (1×) dispersion of ICG NPs (300 μL, 500 μm of net ICG) via tail vein, and the mouse ear was then observed under the NIR-LSCM system. Figure 4a–k shows the NIR microscopic images of ear blood vessels at various vertical depths. Due to bright NIR fluorescence of ICG NPs, the structure of blood vessels could be visualized clearly. Figure 4l shows the corresponding reconstructed 3D image, from which the vascular architecture in the mouse ear was revealed.

3.4 NIR-LSCM imaging of the brain blood vessels in a living mouse

We further performed in vivo brain imaging of 8 week-female ICR mice with the NIR-LSCM system. The skulls of the anesthetized mice were opened up through microsurgery, and the mice were then intravenously injected with PBS (1×) dispersion of ICG NPs (300 μL, 500 μm of net ICG) via tail vein. A thin cover glass was covered on the cranial windows to protect the brain, as well as offer a transparent imaging window. As showed in Fig. 5a–k, the structure of the brain blood vessels at various depths (0–500 μm) could be visualized. A 3D reconstruction was subsequently built (Fig. 5l), and it clearly demonstrated the vascular architecture of mouse brain. Thanks to the low absorption/scattering of NIR excitation and emission light in bio-tissues, deep-tissue observation was achieved by directly utilizing (one-photon) fluorescence confocal microscopy. The average power of the 785 nm-laser after the objective was ∼ 6 mW, which was tolerable compared with the
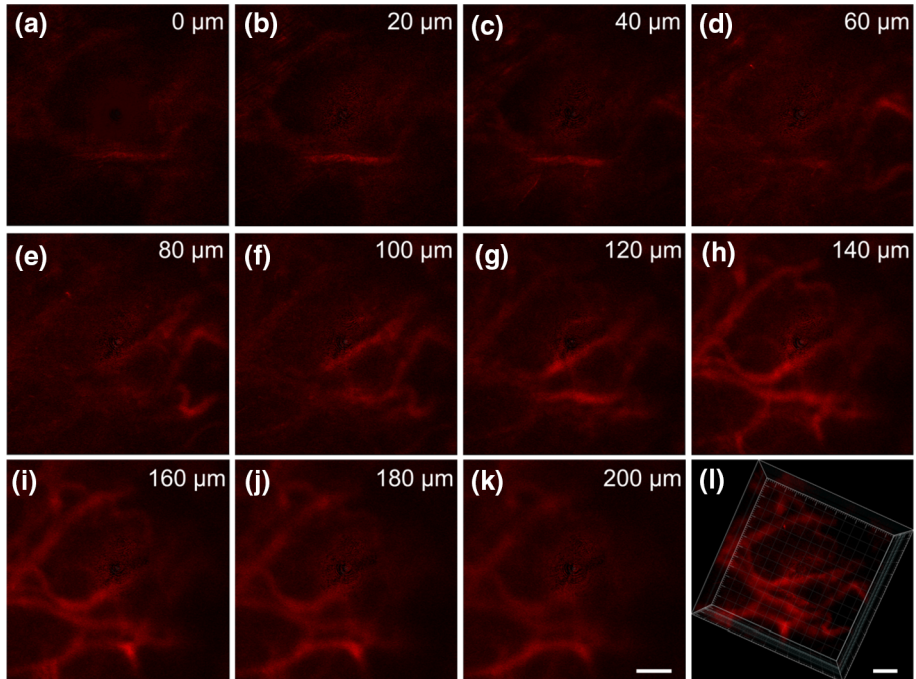
Fig. 4 NIR-LSCM images of blood vessels in the ICG NPs (500 μm) stained mouse ear at various depths **a–k** 0–200 μm. **l** A 3D reconstructed image shows the vascular architecture in mouse ear. Scale bar: 100 μm
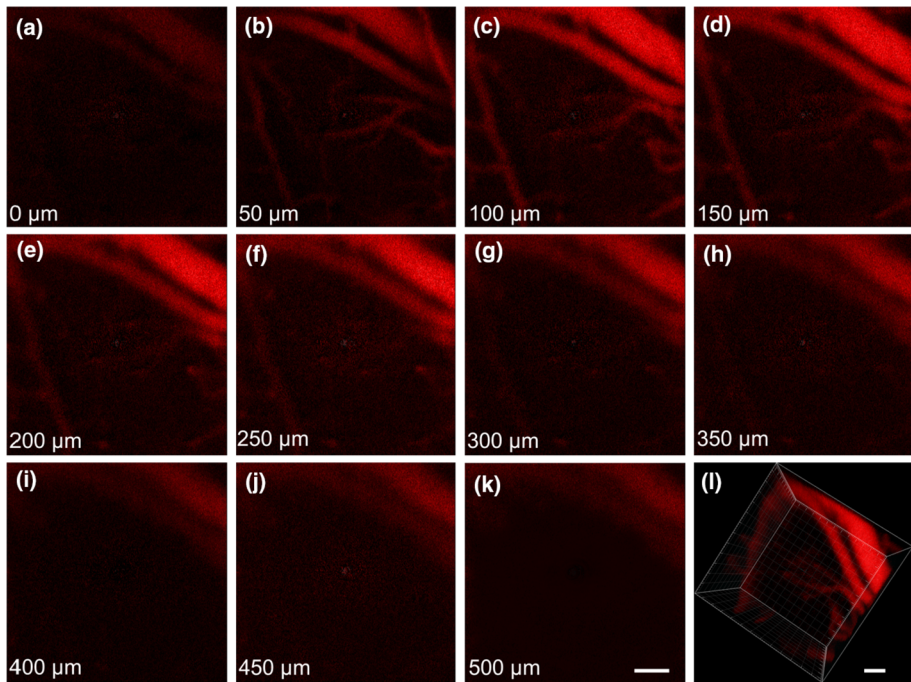
Fig. 5 NIR-LSCM images of blood vessels in the ICG NPs (500 µm) stained mouse brain at various depths **a–k** 0–500 µm. **l** A 3D reconstructed image shows the vascular architecture in mouse brain. Scale bar: 100 µm

excitation power adopted in other in vivo fluorescence imaging applications (O'Connell et al. 2008; Inglefield and Schwartz-Bloom 1997; Grutzendler et al. 2011; Horton et al. 2013). The experimental results further confirmed the feasibility of NPs assisted NIR-LSCM in in vivo bioimaging applications.

However, drawbacks still exist in the present NIR-LSCM system and need to be improved. For example, the NIR-LSCM system was established on a commercial LSCM system (OLYMPUS, FV1000), and the original optical path was optimized on the visible region (380–780 nm) rather than NIR region, which would reduce the efficiency of NIR excitation and the detection of NIR fluorescence signals. Therefore, in the following work, we will optimized the whole optical path, and choose fluorescent NPs with larger absorption and higher quantum yield in NIR region. In addition, we will extend our research to other spectra regions based on the present region (700–900 nm), and find better "window" for NIR-LSCM system applicable to in vivo deep-tissue fluorescence bioimaging.

4 Conclusion

A novel NIR-LSCM system combing the techniques of NIR fluorescence imaging and LSCM was built. In this system, laser source, dichroic mirror and PMT were optimized for NIR excitation and detection. In addition, NIR fluorescent NPs were prepared and utilized as contrast agents for in vivo NIR-LSCM imaging. Fine 3D structure of ear blood vessels

(depth = 200 μm) and cerebral blood vessels (depth = 500 μm) of living mice were obtained successfully. All experiments verified that the NPs assisted NIR-LSCM has great potentials in life science and medicine researches, where deep-tissue and high-resolution microscopic imaging was highly needed.

References

Chu, L., Wang, S., Li, K., et al.: Biocompatible near-infrared fluorescent nanoparticles for macro and microscopic in vivo functional bioimaging. Biomed. Opt. Express **5**(11), 4076–4088 (2014)

Diev, V.V., Schlenker, C.W., Hanson, K., Zhong, Q., Zimmerman, J.D., Forrest, S.R., et al.: Porphyrins fused with unactivated polycyclic aromatic hydrocarbons. J. Org. Chem. **77**(1), 143–159 (2012)

Grutzendler, J., Yang, G., Pan, F., Parkhurst, C.N., Gan, W.B.: Transcranial two-photon imaging of the living mouse brain. Cold Spring Harbor Protoc. **2011**(9), prot065474 (2011)

Hardham, A.R.: Confocal microscopy in plant-pathogen interactions. Methods Mol. Biol. **835**(835), 295–309 (2012)

Horton, N.G., Wang, K., Demirhan, K., Clark, C.G., Wise, F.W., Schaffer, C.B., Xu, C.: In vivo three-photon microscopy of subcortical structures within an intact mouse brain. Nat. Photonics **7**(3), 205–209 (2013)

Huang, X., EI-Sayed, I.H., Qian, W., EI-Sayed, M.A.: Cancer cell imaging and photothermal therapy in the near-infrared region by using gold nanorods. J. Am. Chem. Soc. **128**(6), 2115–2120 (2006)

Inglefield, J.R., Schwartz-Bloom, R.D.: Confocal imaging of intracellular chloride in living brain slices: measurement of gabaa receptor activity. J. Neurosci. Methods **75**(2), 127–135 (1997)

Kim, J.S., Kim, Y.H., Kim, J.H., Kang, K.W., Tae, E.L., Youn, H., et al.: Development and in vivo imaging of a PET/MRI nanoprobe with enhanced NIR fluorescence by dye encapsulation. Nanomedicine **7**(2), 219–229 (2012)

Kim, T.I., Jeong, K.H., Min, K.S.: Verrucous epidermal nevus (VEN) successfully treated with indocyanine green (ICG) photodynamic therapy (PDT). Jaad Case Rep. **1**(5), 312–314 (2015)

Liu, B., Li, C., Chen, G., Liu, B., Deng, X., Wei, Y., et al.: Synthesis and optimization of MoS_2@Fe_3O_4-ICG/PT(IV) nanoflowers for MR/IR/PA bioimaging and combined PTT/PDT/chemotherapy triggered by 808 nm laser. Adv. Sci. **4**(8), 1600540 (2017)

Luo, T., Huang, P., Gao, G., Shen, G., Fu, S., Cui, D., et al.: Mesoporous silica-coated gold nanorods with embedded indocyanine green for dual mode X-ray CT and NIR fluorescence imaging. Opt. Express **19**(18), 17030–17039 (2011)

Ntziachristos, V.: Going deeper than microscopy: the optical imaging frontier in biology. Nat. Methods **7**(8), 603–614 (2010)

O'Connell, M.K., Murthy, S., Phan, S., Xu, C., Buchanan, J.A., Spilker, R., et al.: The three-dimensional micro- and nanostructure of the aortic medial lamellar unit measured using 3D confocal & electron microscopy imaging. Matrix Biol. **27**(3), 171–181 (2008)

Owens, E.A., Lee, S., Choi, J., Henary, M., Choi, H.S.: NIR fluorescent small molecules for intraoperative imaging. Wiley Interdiscip. Rev. Nanomed. Nanobiotechnol. **7**(6), 828–838 (2015)

Ryeom, H.K., Kim, S.H., Kim, J.Y., Kim, H.J., Lee, J.M., Chang, Y.M., et al.: Quantitative evaluation of liver function with MRI using Gd-EOB-DTPA. Korean J. Radiol. **5**(4), 231–239 (2004)

Shi Kam, N.W., O'Connell, M., Wisdom, J.A., Dai, H.: Carbon nanotubes as multifunctional biological transporters and near-infrared agents for selective cancer cell destruction. Proc. Natl. Acad. Sci. USA **102**(33), 11600–11605 (2005)

Tao, H., Yang, K., Ma, Z., Wan, J., Zhang, Y., Kang, Z., et al.: In vivo NIR fluorescence imaging, biodistribution, and toxicology of photoluminescent carbon dots produced from carbon nanotubes and graphite. Small **8**(2), 281–290 (2012)

Treger, J.S., Priest, M.F., Iezzi, R., et al.: Real-time imaging of electrical signals with an infrared fda-approved dye. Biophys. J. **107**(6), L09–L12 (2014)

Uh, H., Petoud, S.: Novel antennae for the sensitization of near infrared luminescent lanthanide cations. C. R. Chim. **13**(6–7), 668–680 (2010)

Webb, R.H.: Confocal optical microscopy. Rep. Prog. Phys. **59**(3), 427–471 (1996)

Weissleder, R.: A clearer vision for in vivo imaging. Nat. Biotechnol. **19**(4), 316–317 (2001)

Welsher, K., Liu, Z., Daranciang, D., Dai, H.: Selective probing and imaging of cells with single walled carbon nanotubes as near-infrared fluorescent molecules. Nano Lett. **8**(2), 586–590 (2008)

Welsher, K., Liu, Z., Sherlock, S.P., et al.: A route to brightly fluorescent carbon nanotubes for near-infrared imaging in mice. Nat. Nanotechnol. **4**(11), 773–780 (2009)

Welsher, K., Sherlock, S.P., Dai, H.: Deep-tissue anatomical imaging of mice using carbon nanotube fluorophores in the second near-infrared window. Proc. Natl. Acad. Sci. USA **108**(22), 8943–8948 (2011)

Yang, F., Murugan, R., Wang, S., Ramakrishna, S.: Electrospinning of nano/micro scale poly (L-lactic acid) aligned fibers and their potential in neural tissue engineering. Biomaterials **26**(15), 2603–2610 (2005)

Yodh, A., Chance, B.: Spectroscopy and imaging with diffusing light. Phys. Today **48**(3), 34–40 (1995)